The Effects of pH and Ionic Strength on Protein Adsorption of Lysozyme and Bovine Serum Albumin to a Silicon Oxide Interface

Thomas J Leyshon

University of Manchester

Abstract

Understanding the key mechanisms that dictates protein adsorption stirs great interest and intrigue amongst many. Proteins and their amino acid counterparts perform many important physiochemical reactions that provide and sustain life. Demystified the complex nature behind the crucial physiochemical processes associated with protein adsorption could revel new biological, medical or technological advancements. Through the use of Spectroscopic Ellipsometry and an accompanying computer simulation, the effects on protein adsorption within an aqueous media on to silicon oxide was examined for varying pH and ionic strengths. Two proteins were examined, lysozyme and BSA. The experimental results proved to be reproducible. The results agreeing with both previous experimental findings and our initial hypothesis. The accompanying simulation model was produced in an attempt to replicate and reinforce the experimental findings. The model was built upon both theoretical and experimental adsorption literature. The model produced reasonable results for lysozyme however not for BSA, reasons behind this discrepancy are explored. This report serves as a strong basis to further develop a simulation model that makes accurate and realistic predicts of the the experimental observations in protein adsorption.

Keywords: Biophysics, Protein Adsorption, Experimental, Computational

1. Introduction

Protein adsorption at the solid-liquid interface occurs over a wide range of chemical environments. Biointerface interactions are prevalent in nature and their crucial roles in many important phenomena spurs intensive research interests and efforts in the medical, pharmaceutical and food processing fields. Understanding how the protein kinetics vary under chemical changes and how the overall protein adsorption for different initial conditions are important topics [1]. Solving these unknowns associated with protein-interface binding could prove to reveal crucial information in topics concerning an array of issues, including both disease recognition and prevention [2]. Lysozyme and BSA are both globular proteins, which are complex biological molecules [3]. Examinations of the dynamic adsorption of lysozyme and BSA between a PBS buffer - silicon oxide interface subjected to varying pH and ionic strengths were undertaken. Measurements were taken using in situ spectroscopic ellipsometry. Ellipsometry is one of a handful of techniques that can be used for examining protein adsorption. For this experiment ellipsometry was the most appropriate technique for this project. Due to it being fairly inexpensive as well as being a non-perturbing optical technique (it does not require the excitation of, nor the alternation of the proteins). As ellipsometry involves only relative amplitudes and relative phase measurements, it is highly accurate, it is also capable of accurately detecting minute by minute changes on the interface [4]. A substantial amount of literature has already been produced on lysozyme and BSA adsorption for a wide range of substrates. Their basic information (molecular weights, isoelectric points) and general behavior are well established. This project still bears importance in replicating and further solidifying our knowledge on their behaviors. The project also provided a basis for developing a new and versatile computational model to predict protein adsorption [5].

2. Ellipsometry

2.1. Theory

2.1.1. The principles of Spectroscopic Ellipsometry

Ellipsometry has a number of advantages. Whilst neutron source techniques are expensive and access to facilities is limited, ellipsometry is easy and relatively inexpensive to use. Ellipsometry offers useful structural information. Spectroscopic ellipsometry differs from the conventional null ellipsometry in that it has the flexibility to perform measurements over a wide

range of wave lengths, this increases the sensitivity of the interfacial structural recordings [6]. The typical range of film thicknesses in which an ellipsometry method is used, lies between the sub nanometers to the micron level. In ellipsometry a collimated beam of monochromatic light is polarized in a known state. This beam is incident upon the subjected sample, the reflected light beam that is produced is than analyzed [9]. Maxwells equations of light dictate that when light interacts with a material the law of reflection and certain boundary conditions must be conserved. These boundary conditions are mathematically described by Snells law

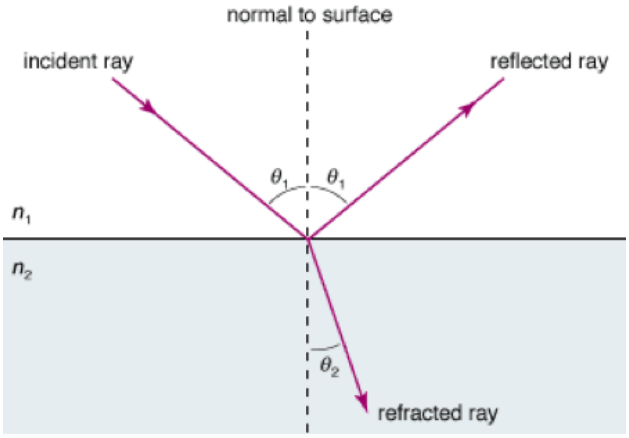

Figure 1: Snell's law illustration [7]

$$n_i \sin\theta_i = n_t \sin\theta_t \tag{1}$$

where n is the the refractive index and represents the angle to the normal of the surface. The subscript and refer to the incident and transmitted beams of light respectively. These parameters are illustrated in figure 1. The boundary conditions can be used to determine the electric fields parallel and perpendicular to the sample surface. The light beam can then be separated into orthogonal components with relation to the plane of incidence. These electric fields which are perpendicular and parallel to the incident plane are known as the p and s polarized planes, respectively. They are shown below in figure 2. The Fresnel equations stem from Snells law and describe light when it moves between two different refractive indexed media. These equations

predict the light that will be reflected off the boundary back into the 1st media, Fresnel reflection [8].

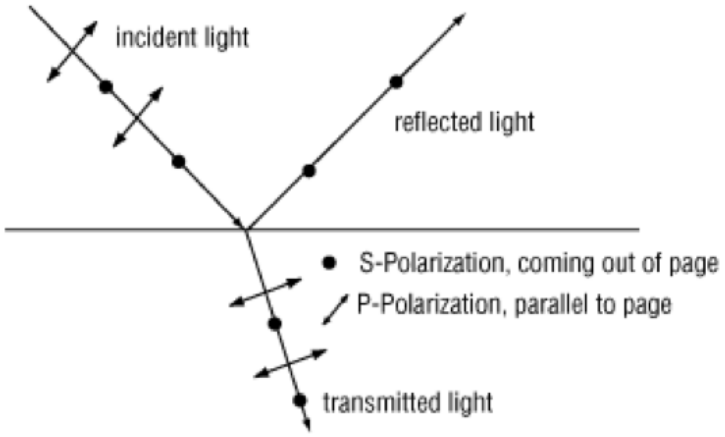

Figure 2: Polarized light illustration [8]

Due to the conservation of energy, two equations arise relating the transmittance, and reflectance, of each individual polarized plane, as seen in equation 2 and 3.

$$T_s = 1 - Rs \tag{2}$$

$$T_p = 1 - Rp \tag{3}$$

2.1.2. Detection & Analysis process

Ellipsometry takes advantage of the polarization of light beams and the boundary conditions in which light must obey. As the light beam enters the material it undergoes a change in velocity due to refraction. The amount of refraction caused to the light is dependent on the materials properties [9]. When the transmitted light reaches the other side of the thin film it will undergo another reflection/refraction this time at the thin film substrate interface. This is illustrated in figure 3. The reflected light of the substrate interface will be subjected to travel back through the film and encounter the thin film surrounding environment interface. The light that travels back

into the surrounding environment will cause superposition with the originally reflected light. These multiple light waves create an interference pattern that will be dependent of each relative phase of the light waves alongside the original reflected light beam. The relative phase of each light component can be used to determine the overall reflected or transmitted beam [9].

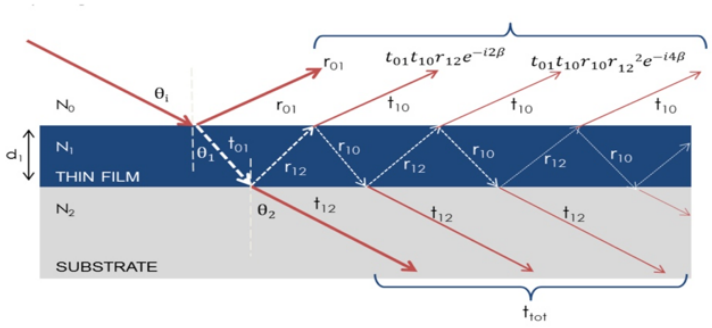

Figure 3: Thin film analysis [9]

The p and s components will be subject to change in respect to each other upon reflection. The change in polarization can be described using two parameters, ψ and Δ. These parameters are what are used in ellipsometry to analysis data. Equation 4 shows the relationship of the two parameters [9].

$$\rho = \tan \Phi e^{i\Delta} \tag{4}$$

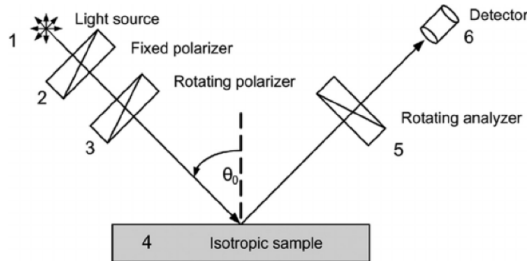

Figure 4: Simple schematic diagram of the components in an ellipsometer [10]

Figure 4 is a simple schematic diagram of the primary features of an ellipsometer, comprising of an initial component to polarize light into both s and p planes. A surface plate to hold the sample in place is in the center of the ellipsometer. The light is reflected off the sample and into the rotating analyzer (RAE), how much light passes through the RAE into the detector is dependent on the polarizer orientation. The light collected by the ellipsometer detector, is transformed into an electrical signal. From this electrical signal the specific polarization of the light beams can be determined. The polarization of the reflected light in comparison to the polarization of the incident light is what governs the values of ψ and Δ [9]. Once ψ and Δ have been distinguished, the parameters are compared to preexisting models which reveal the thickness of the films. The process of regression is used to find the best fit between experimental data and a model. The unknown parameters are allowed to vary within the Mean Squared Error values [9]. Using a dispersion relationship of all wavelengths, the optical constants n and κ are determined. The Cauchy relationship is adjusted accordingly to fit the refractive index for the material [9].

2.1.3. Protein properties and the adsorption layer

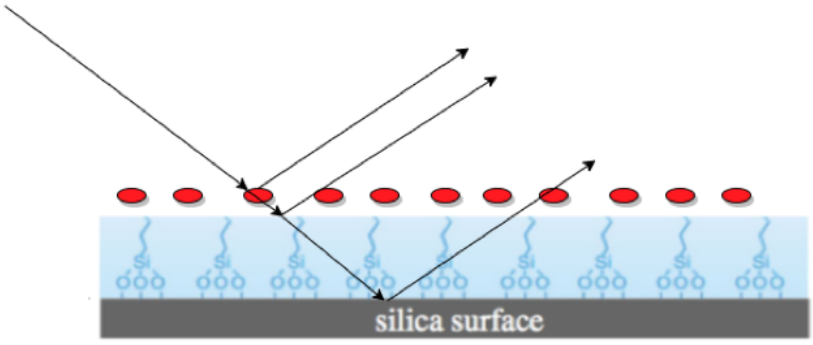

Figure 5: Reflection off protein adsorption to silicon oxide layer

Figure 5 shows an ellipsometer detecting the thickness of the adsorbed protein layer. The two proteins that will be used in this experiment are Lysozyme and BSA. Lysozymes primary function is the hydrolysis of heterpolymers in bacterial cell walls. It is a common antibacterial agent which is found in pathogen protective fluids such as mucus. Lysozyme is a small globular protein with a mass of $14,300Da$. Its globular structure is roughly ellipsoidal and has an approximate dimension of $303045\mathring{A}$[5]. It has a significant alpha helix and beta sheet structures, as seen in the figure 6. Lysozyme is positively charged at neutral pH and its isoelectric point pH is 10.7. This isoelectric point corresponds to a zero zeta potential as the protein (net charge of zero) will remain stationary in an electrical field [2]. BSA is a protein rich in disulfides, 17 disulfide bonds. These bonds significantly alter its stability and adsorption dynamics. BSA is a large globular protein with a mass of $66500Da$. BSA is known to have good ion, fatty acid and hormone binding capacities [2]. Its isoelectric point is around pH 4.8, and the globular dimension are about $4040140\mathring{A}$ [5]. BSAs residue structure is shown in figure 6.

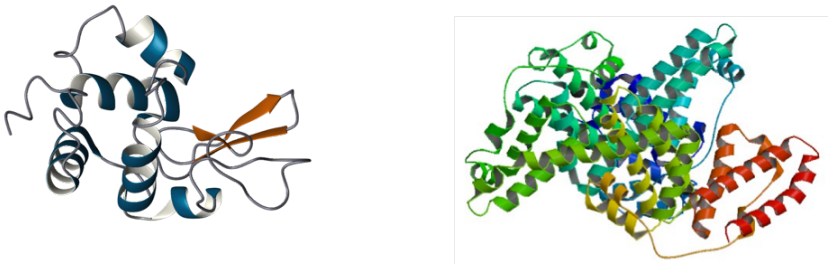

Figure 6: Structure of lysozyme (left) and structure of BSA (right) [11]

2.2. Experimental Method

2.2.1. Materials

A Silicon wafer was purchased from Compact Technology Ltd, this was cut into individual 12mm x 12mm squares. The Phosphate-buffered saline (PBS) solutions were produced from Na_2HPO_4 and NaH_2PO_4 (Sigma, UK) and ultra-high quality (UHQ) water. An ionic strength and pH calculator were used to determine the required concentrations (had to be adjusted for UHQ water being pH 6 not 7), a research quality weighing scale was used, with an uncertainty of 0.01mg. Decon90 solution was purchased from Decon Laboratories Limited, East Sussex, UK. Bovine serum albumin (BSA) and Lysozyme from chicken egg white were purchased from Sigma-Aldrich, UK. Chicken egg white lysozyme (Sigma, 99%+, catalog no. L6876) was used as supplied. BSA (Sigma, catalog no. A0281) was fatty acid-free and was also used as supplied [5]. Silicon is widely used as a common biointerface substrate, as it can be polished to give a very smooth surface. As well as a silicon substrate has a layer of native oxide on the surface. Silicon substrate has a high refractive index which causes a large optical contrast with an organic layer, such as protein [4]. The Silicon wafers were initially rinsed and cleaned using a 5% Decon90 95% UHQ water solution, then dried with hot air. this was to remove all impurities from the wafers surface, producing a hydrophilic uniform silicon oxide layer with a thickness of 12 1 Å. This cleaning procedure was undertaken before every reuse of the substrate.

An (AJ. Woolam M-2000) ellipsometer, along with completeEASE software was used to measure, determine and record the static interface film thickness data and the in situ dynamic adsorption data. All measurements were made at an incident angle of 70 degrees to the normal. A Teflon sample cell fitted with 2 quartz windows and a volume of 3ml along with a plastic

insert were used to hold the silicon wafer in place whist accommodating the PBS and protein solutions. Disposable glass pipets were used to inject the various solutions into the sample cell.

2.2.2. Procedure

9 measurements equally separated across the area of the wafer were made of the native silicon oxide layer, this was to check the uniformity of the layer was $12 \pm 1\mathring{A}$. If the Silicon wafer had a uniform silicon oxide layer of $12 \pm 1\mathring{A}$, then it was placed within the sample cell. Initial ellipsometry measurement were made to determine the window parameters of the cell, these were needed to calibrate the measurements within the cell. PBS solutions were injected using glass pipets, measurements of the buffer silicon oxide interface were undertaken. The PBS buffer was then subject to in situ measurements until it reached a stable equilibrium within $\pm 3\mathring{A}$ of the zero-point position, the cut off time for this process was 10 minutes. After 10 minutes the PBS buffer was removed and replace with the corresponding (same ionic and pH strength) protein PBS solution. The protein solutions were left until they plateaued and reached an equilibrium state, this occurred within an hour, therefore a cut off time of 1 hour was used to complete this process. After this time the protein buffer was then removed and replaced with the original PBS solution and left for 10 minutes, this was to observe the amount of desorption from the interface. The amount of initial desorption provides information about the proportion of irreversibly and reversibly adsorbed proteins to the interface.

2.2.3. Measurements

Measurements of the effects of varying protein concentration on adsorption were undertaken first. These consisted of six variations of protein concentration solutions for both Lysozyme (ranging from 0.001 to $0.2mgml^{-1}$) and BSA (ranging from 0.02 to $1mgml^{-1}$). The pH effect on protein adsorption was than examined, 2 lysozyme concentrations and 2 BSA concentrations at fixed ionic strength of $20mM$ were subject to 5 variations of pH concentration ranging from pH 5.03 to pH 8.3. Finally, the ionic strength effect on protein adsorption was carried out on 2 lysozyme concentrations and 2 BSA concentrations. 3 ionic strengths were tested at a fixed pH of 7, consisting of 4, 20 and $100mM$ strengths.

The selection of different protein concentrations used was chosen through the comparison of the molecular densities of the two proteins. As BSA is around 5 times heavier than lysozyme, to achieve roughly same molecular

densities of each protein BSA concentrations needed to be 5 times that of lysozyme. The pH and ionic variations were chosen to be spread across either sides of the physiological and neutral values, ranging from pH 5 to pH 8.3. The temperature in which all experiments were taken was kept constant at room temperature, $293 Kelvin$, a thermostat regulated temperature throughout.

3. Simulation

3.1. Motivation

In order to truly understand the physical behavior of protein adsorption the underlying microscopic molecular interactions and kinetics must be comprehended. If successfully undertaken computer simulations are very power tools. If a simulation of Lysozyme and BSA adsorption can successfully predict adsorption under changing pH and ionic strength, then this could be the basis to analyse more advanced adsorption phenomena, that would be very difficult to investigate in the laboratory. The power of simulation is that these predictions can be made without having to use any experimental equipment nor waste any materials. MatLab 2015 was used to script and programme the model. The style of programming was hierarchical, alternating between three main scripts $ad\_model\_ionic, ad\_model\_pH and ad\_model\_concentration$. Inheritance was used to separate particularly large functions in individual classes. The programme was formatted to have an efficient runtime. Vectorization was used whenever appropriate. The programme can simulate protein adsorption between pH values of 6.75 to 11.4, within a temperature of 273 to 373 kelvin. Surface parameters of water, silicon oxide, BSA and lysozyme were taken from (Hofmeister, 1997), (Van Oss, 1996) and (Spielman & Friedlander,1973). This simulation assumed each individual globular protein to be a sphere of uniform density with no orientation preferences or ability to deform [13].

3.2. Theory

3.2.1. Gibbs Free Energy & Statistical Analysis

Gibbs free energy is a thermodynamic potential. The potential is used to calculate the maximum or reversible work that is available within a thermodynamic system. The Gibbs free energy of a system may be the sum of many different contributors. In an isolated system Gibbs free energy is given by

$$\Delta G = -T\Delta S \tag{5}$$

where is the fixed temperature of the system and is the change in entropy of the system. Gibbs free energy is most useful for thermochemical processes at constant temperature and pressure [14].

3.2.2. Energetics & Molecular Dynamics

When a macromolecule approaches an interface 3 sets of parameters describing the interfacial energy must be considered, the absorbent (Silicon Oxide layer, 1), the macromolecule (the protein, 3) and the liquid (the PBS buffer solution, 2). The energies for these three phases increase and decrease, giving rise to repulsion or attraction respectively. The energetics are 8 created from a combination of three main contributions that occur between biological and non- biological macromolecules, surface and particles [15].

- Electrodynamic, Lifshitz Van der Waals (LW) interactions. These are the weak electrostatic attractive forces created by the electric dipole moment between uncharged molecules. [15].
- Polar, electron donor & acceptor (da) (Lewis acid-base (AB)) interactions. This is the donating of an electron from one molecular to another. This is important and has dominant effects in ligand binding [15].
- Electrostatic (el) interactions. Essentially another Van der Waals force, which arise from opposite charged ions attract [15].

3.2.3. DLVO Theory

DLVO theory can be used to explain the aggregation of the proteins in an aqueous solution. It is used to determine key parameters associated with the forces between charged surfaces within an aqueous medium. DLVO does this by combining the effects of both the attractive Van der Waals and the double layer electrostatic repulsion between counter ions [16].

1. Van der Waals attraction -

   The net interaction energy for a molecule at a distance D from the surface is given by

$$W(r) = -2\pi C\rho_1 \int_D^\infty dz \int_0^\infty \frac{x}{(z^2+x^2)^3} dx \tag{6}$$

$$W(D)_A = \frac{2\pi C\rho_1\rho_2}{12} \int_0^{2R} \frac{(2R-z)z}{(D+z)^3} dz \approx \frac{\pi^2 C\rho_1\rho_2 R}{6D} = -\frac{AR}{6D} \tag{7}$$

$$A = \pi^2 C\rho_1\rho_2 \tag{8}$$

Where W(r) is the interaction energy of the molecule and the surface, E is the number density of the surface, T is the number density of the sphere, z is the axis perpendicular with the surface and originates at the molecule, D is the z position of the surface, x is the axis perpendicular with z axis. A is known as the Hamaker constant [17].

2. Double layer force -

As the Silicon Oxide surface adsorbs the charged molecules from the surroundings it will develop a wall surface potential that will attract counter ions whilst repelling co ions. The region of increased counter ion attraction is known as the electrical double layer. This region can be distinguished as two different layers. The Stern layer which is closest to and strongly bound to the surface [17]. A diffuse layer lies on top of this initial Stern layer. This diffuse layer causes electrostatic screening of the wall charge, which reduces the Gibbs free energy of the electrical double layer [16]. Figure 8 illustrates these layers. The Debye screening length $\frac{1}{\kappa}$ describes the thickness of the diffuse layer. κ is given by

$$\kappa = \left(\frac{\sum_i \rho_{\infty i} e^2 z_i^2}{\epsilon_r \epsilon_0 k_b T}\right)^{\frac{1}{2}} \tag{9}$$

where $\rho_{\infty i}$ is ion i's number density in the bulk solution and z is the ions valence. γ represents the surface potential and is determined by the equation 9, Ψ_0 is the potential on the surface [17].

$$\gamma = \tanh \frac{e\psi_0}{4kT} \tag{10}$$

Once values for κ and γ have been obtained the free energy associated with the electrostatic repulsion between two spheres of radius R can be calculated using

$$W(D)_R = \frac{64 k_b T R \rho_\infty}{\kappa^2} e^{-\kappa D} \tag{11}$$

Combining the attractive Van der Waals interaction energy and the repulsive double layer interaction energy produces the total interaction energy $W(D)$.

$$W(D) = W(D)_A + W(D)_R \tag{12}$$

3. ζ potential -

The ζ potential is the electro-kinetic potential of the system, it is the potential difference between the dispersion medium and the stationary layer of fluid surrounding the molecule [17]. The potential cant be measured directly but it can be determined either by measurements of electrophoresis or theoretically using the LinderstrmLang equation [18]. ζ potential values for lysozyme and BSA were already experimentally determined in previous literature [19]. The ζ potential is important in relating the effects of pH and ionic strength changes in terms of the electrostatic forces of the system. Figure 7 shows the distance dependence of the ζ potential and the positions of the stern layer and slipping plane.

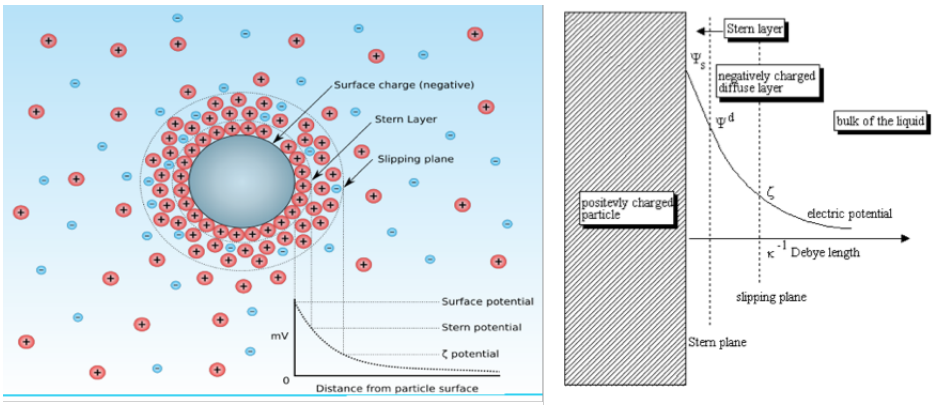

Figure 7: Illustration of the diffuse layers of a molecule, showing the zeta potentials distance dependence [20]

The self-diffusion coefficients of water must then be calculated and set for a fixed temperature. A best fit was produced between temperature

and self-diffusion coefficients in which the user could now extract the self-diffusion coefficient for any temperature desired.

4. Interfacial surface tensions, γ_i -

The specific interfacial free energy has units of energy per unit area. Equivalent to force per unit length and simply the surface tension, γ. The first step in calculating the interfacial free energy, γ_{123} in the presence of solvent is characterizing the energetics of the adsorption process [18]. The three surface tensions corresponding to the three energy components, LW, el and da were found for each media; protein (3^{rd} component), solution (2^{nd} component) and adsorbent (1^{st} component). These combine to form ΔG_{123}, the change in overall Gibbs free energy of the system [18].

$$\Delta G_{123} = \Delta G_{123}^{LW} + \Delta G_{123}^{da} + \Delta G_{123}^{el} \tag{13}$$

The donor acceptor forces dominate ΔG_{123}, contributing to about 80-90% of the total interfacial energy, while LW and el only account for around 5-10%. The equations used to define these individual interfacial energies in terms of the surface tensions are

$$\Delta G_{12}^{da||} = -2[(\gamma_2^+\gamma_1^-)^{\frac{1}{2}} + \gamma_1^+\gamma_2^-)^{\frac{1}{2}}] \tag{14}$$

For the da force electron donors ($-$) and acceptors ($+$) both contribute to the interfacial energy, donor and acceptor surface tensions for the 1^{st} and 2^{nd} media are combined to make an overall γ_{12}^{da}

$$\gamma_1^{da}2 = 2(\sqrt{\gamma_1^+} - \sqrt{\gamma_2^+})(\sqrt{\gamma_1^-} - \sqrt{\gamma_2^-}) \tag{15}$$

To take account of the distance dependence of the interfacial free energy that corresponds to the potentials felt between the protein and surface on approach. An adsorption rate coefficient defined as

$$\kappa_a = \frac{D}{\delta_a} \tag{16}$$

where the distance δ_a is defined as

$$\delta_a = \int^{\infty} [e^{\frac{\Delta G(z)}{kt}} - 1]dz \tag{17}$$

the final LW, da and el distance dependent interfacial energies are given by

$$\Delta G^{LW} = \frac{2\pi l_0^2 \Delta G^{LW||} r}{z} \tag{18}$$

$$\Delta G^{el} = 4\pi\epsilon_0\epsilon\psi_1\psi_3 \ln 1 + e^{-kz} r \tag{19}$$

$$\Delta G^{da} = 2\pi\chi\Delta G^{da||} e^{\frac{(l_0 - z)}{\chi}} r \tag{20}$$

These equations are applicable to adsorption, of a spherical protein approaching a planar surface, where χ is the decay length of the donor-acceptor interactions. ψ_1 was determined from the Healy & White model (1978), a hill climb programme was scripted to find ψ_1. The zeta potential, ζ already determined was used as an estimate for ψ_3 [21]. From this the total Gibbs free energy of the system was determined.

The Maxwell method models the particles as reversibly attached to an adsorbent when they get trapped in the secondary energy minimum, ΔG_{min2} [16]. The Gibbs free energy and the potential energy-distance landscape between the protein and silicon-oxide layer has already been established using DVLO theory. The next step in the Maxwell method is to determine the potential barrier height of the adsorbent substrate and escape probability of the reversibly attached proteins. This method assumes the proteins kinetic energies are dictated by the Maxwell distribution function [16]. It is assumed that the proteins can be modelled as an ideal gas, the root mean square velocity was than determined from the equation

$$v_{rms} = \sqrt{\frac{3k_bT}{m}} \tag{21}$$

The kinetic energy associated with this velocity can be calculated via

$$E_{kin} = \frac{1}{2} m v_{rms}^2 \tag{22}$$

The Interaction Force Boundary Layer (IFBL) model was used to calculate the sticking Efficiency, α , this is defined as the proportion of particles that collide with the interface that remain attached.

$$\alpha = 1 - \int_{-\Delta G_{min2}}^{\infty} f(E_{kin}) dE_{kin} \tag{23}$$

where

$$f(E_k in) = \frac{2}{\sqrt{\pi} k_b T} \sqrt{\frac{E_{kin}}{k_b T}} e^{-\frac{E_{kin}}{k_b T}} \tag{24}$$

Along with the sticking efficiency the collision efficiency was also determined via the Smoluchowski-Levich equation. The collective efficiency is the product of the collision efficiency and the sticking efficiency. The collective efficiency is therefore defined as the amount of particles that collide with the absorbent and then stick to it [16]. The escape rate of proteins per a second can be calculated by comparing the number of proteins with enough energy to escape the potential barrier of the secondary minimum. The collision frequency with this potential barrier is defined and the required escape velocity is given by

$$v_{esc} = \sqrt{\frac{2E_b arrier}{m}} \tag{25}$$

where $E_{barrier}$ is the 2^{nd} minimums potential energy barrier and m is the mass of the protein. The escape probability is the probability that a protein will have a velocity greater than or equal to this escape velocity. This is determined by a Maxwell-Boltzmann distribution at room temperature. Each iteration of the model correlated to a time period of 0.0001 seconds.

The simulation plotted the potential energy-distance landscape between the protein and silicon-oxide layer, shown in figure 8. from this plot the secondary energy minimum, ΔG_{min2} and its potential energy barrier was determined.

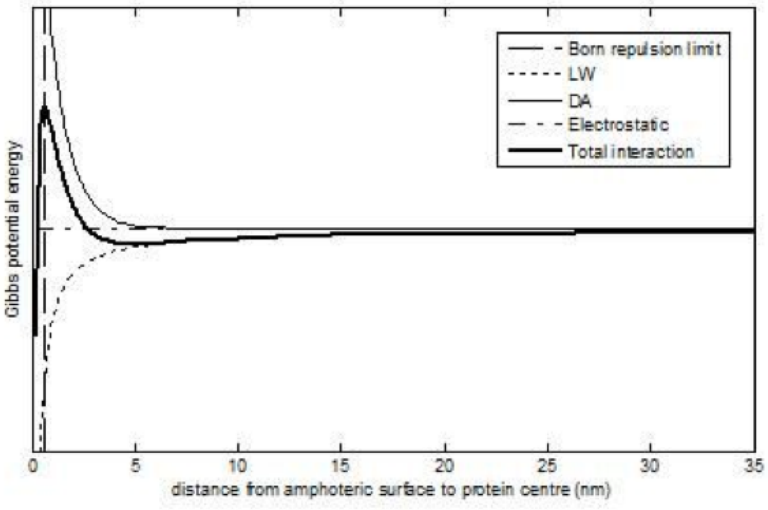

Figure 8: Gibbs potential energy vs distance silicon oxide surface to protein

The adsorption amount, Q could now be expressed as

$$N_0 = \frac{(protein\,flux)(collection\,efficiency)(wafer\,area)(iteration\,time)}{protein\,mass} \tag{26}$$

and the fractional protein coverage of the substrate could be expressed as

$$Fraction\,surface\,coverage = \frac{N_0}{N_{max}} \tag{27}$$

.The above methodology was scripted and programmed in MatLab and graphs of the fractional surface coverage of protein on the substrate vs time were produced for variation of pH, ionic strength and protein concentration.

4. Results & Discussion

4.1. Ellipsometry

4.1.1. Protein Concentration Effect

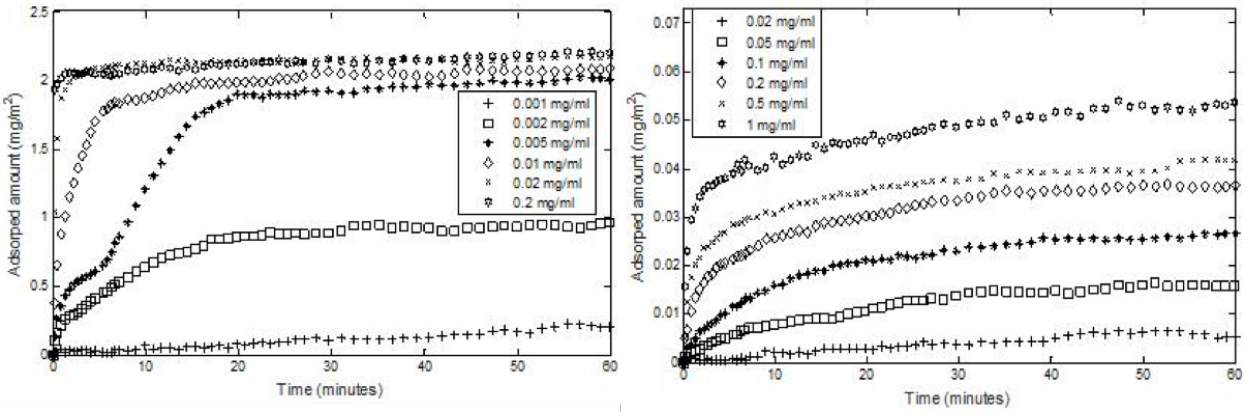

Figure 9: Protein concentration effect, lysozyme (left) and BSA (right)

Figures 9 shows the adsorbed amount of protein in mgm^{-2} on to silicon oxide for varying protein solution concentrations. The general trend of exponential increase within the first few minutes of exposure can be seen in both lysozyme and BSA. However, lysozyme adsorption is substantially higher for smaller concentrations. A comparison of adsorption at a concentration of $0.2mgml^{-1}$ can be made. At this concentration BSA has a relatively minuscule coverage of the interface which peaks at a value 0.06 mgm^{-2} after 45 minutes. Whilst lysozyme at this concentration had adsorption and plateaued at a coverage value of 2.1 mgm^{-2} within the first 5 minutes of protein solution exposure.

For lysozyme the data suggests there is at upper limit to the amount of adsorption that can occur on to a silicon oxide layer. A twenty-fold increase of lysozyme concentration from a value of $0.01mgml^{-1}$ to $0.2mgml^{-1}$ brings an increase of less than $0.1mgm^{-2}$ in the overall adsorbed amount. However, for BSA, the increase of protein concentration seems to correlate to a consistent increase in adsorbed amount. This suggests that the upper limit of BSA adsorption on a silicon oxide layer was not reached, even with much greater concentrations being tested than for lysozyme. The data

shows a clear contrast in the adsorption affinity between the two proteins, with lysozyme having the higher affinity for binding to the interface.

4.1.2. The pH Effect

1. Lysozyme

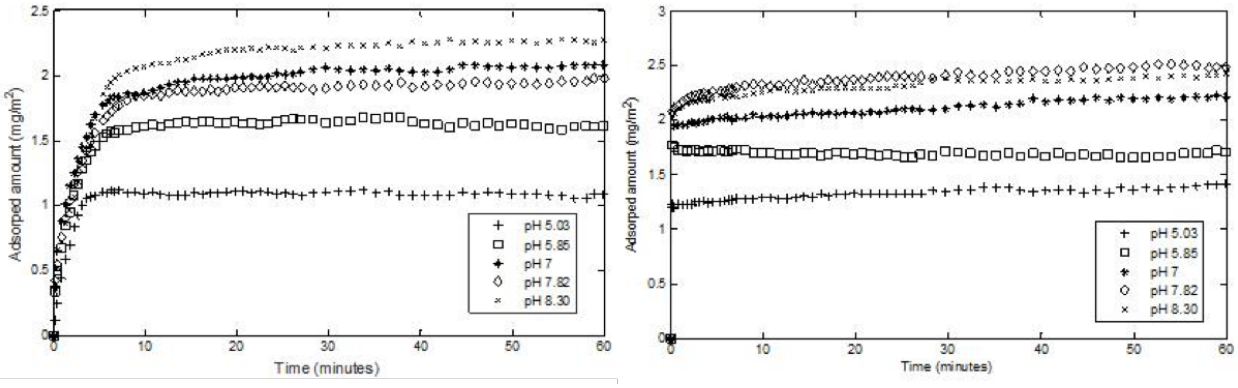

Figure 10: pH Effect upon lysozyme concentrations 0.01mgml (left) and 0.1mgml (right)

A positive correlation generally exists between an increases in pH strength and an increase in lysozyme adsorption. The general trend is present in both 0.01 and 0.1 $mgml^{-1}$ protein concentrations, this can be seen in figure 10. Although the effects were less prominent in the 0.1 $mgml^{-1}$ concentration. For the 0.01 $mgml^{-1}$ concentration the greatest adsorption was seen at a pH of 8.3. However, the 0.01 $mgml^{-1}$ data shows a preference towards pH 7.0, this was the only concentration that had a higher adsorption rate than the next increased pH concentration (pH 7.8). For 0.1 $mgml^{-1}$ concentration the general trend of increased pH causes an increase in adsorption is still up to pH 7.0, the highest adsorption was observed at a pH of 7.8.

2. BSA

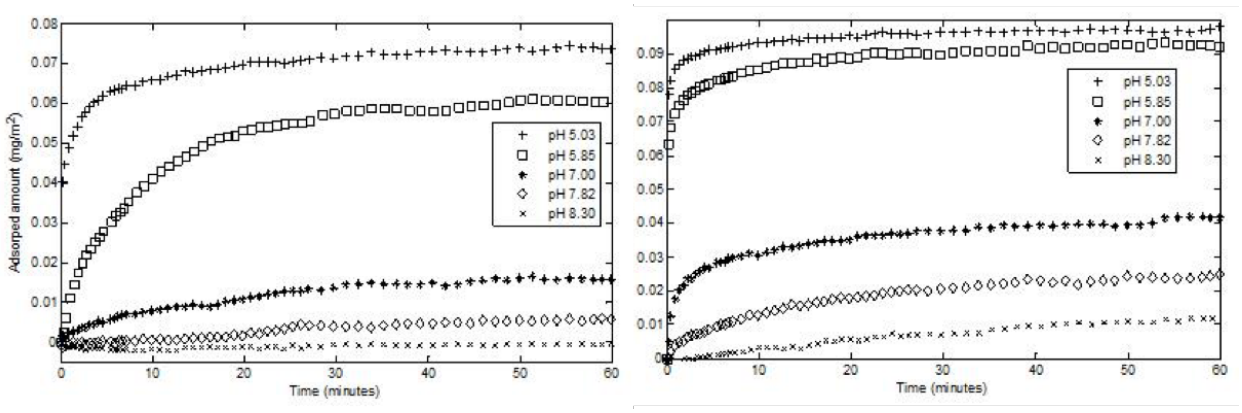

Figure 11: pH effect upon BSA concentrations, 0.05 mgml (left) and 0.5 mgml (right)

Compared to lysozyme adsorption the opposite correlation was observed for BSA, see figure 11. An increase in pH causes a decrease in absorbed amount. This trend was present in both BSA concentrations. The trend was consistent across all 5 pH variations, an increase in pH always corresponded to a decrease in adsorption. However, the largest difference in adsorption amount in both BSA concentrations was observed between pH 7.0 and pH 5.85 solutions.

4.1.3. Ionic concentration effect

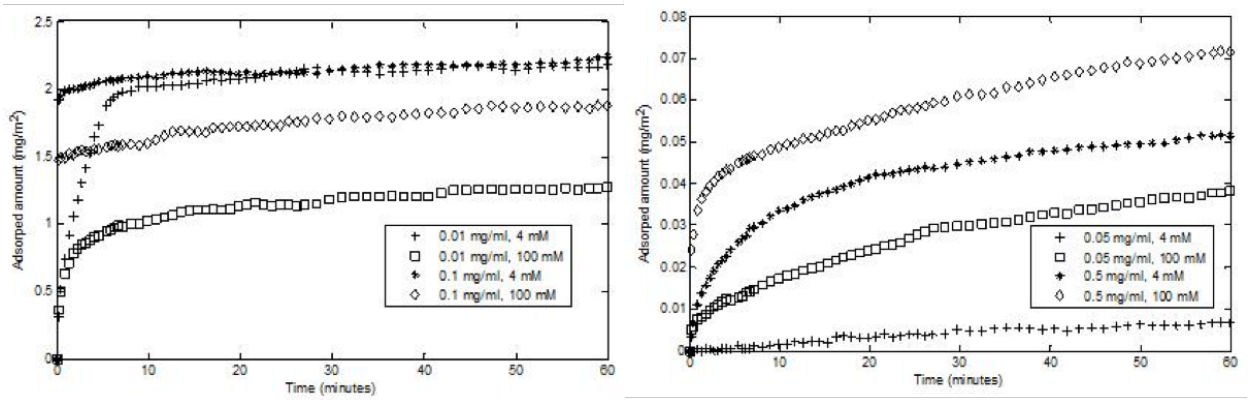

Figure 12: Ionic effect upon lysozyme (left) and BSA (right)

An increase in ionic concentration correlates to a substantial decrease upon lysozyme adsorption for a lysozyme concentration of $0.01 mgml^{-1}$. An increase in ionic concentration results in a decrease in lysozyme adsorption is also present for a Lysozyme concentration of $0.1 mgml^{-1}$, however the effects are less prominent than in $0.01 mgml^{-1}$. Compared to lysozyme adsorption the opposite correlation was observed for BSA. For BSA an increase in ionic strength correlated to an increase in overall BSA adsorption. This correlation can be seen in figure 12 and is more prominent for the lower concentration of BSA, $0.05 mgml^{-1}$.

4.1.4. Ellipsometry Error Prevention & Analysis

Reducing the systematic errors within the data was considered in all areas of the experiment. Keeping the same orientation and position of the silicon wafer substrate was deemed important as this would improve the consistence across all measurements taken. Pencil markings were made on the ellipsometer sample disk as well as a small marking was made on both the silicon wafer and the sample cell to ensure the same orientation of these components. Cleaning, rinsing and drying of both the sample cell and the silicon wafer was undertaken after each protein adsorption measurement. The cleaning process is described in the experimental procedure section. Latex gloves and a lab coat were worn at all times to ensure the equipment and solution

was not contaminated by material fibers. Air and water calibration measurements were made before beginning the experiment to ensure the sample cell and apparatus gave consistent accurate recordings. The ellipsometer produced extremely precise, results each reading had an associate error between $\pm 0.6\mathring{A}$.

4.2. Simulation

The results produced from the simulation consist of protein concentration effect, the pH effect for 2 variations of protein concentration and the ionic effect for 2 variations of protein concentration. The data was produced for lysozyme only, an error occurred in the BSA results. This error is thought to of stemmed from an incorrect BSAs zeta potential used in the model.

1. Protein Concentration Effect

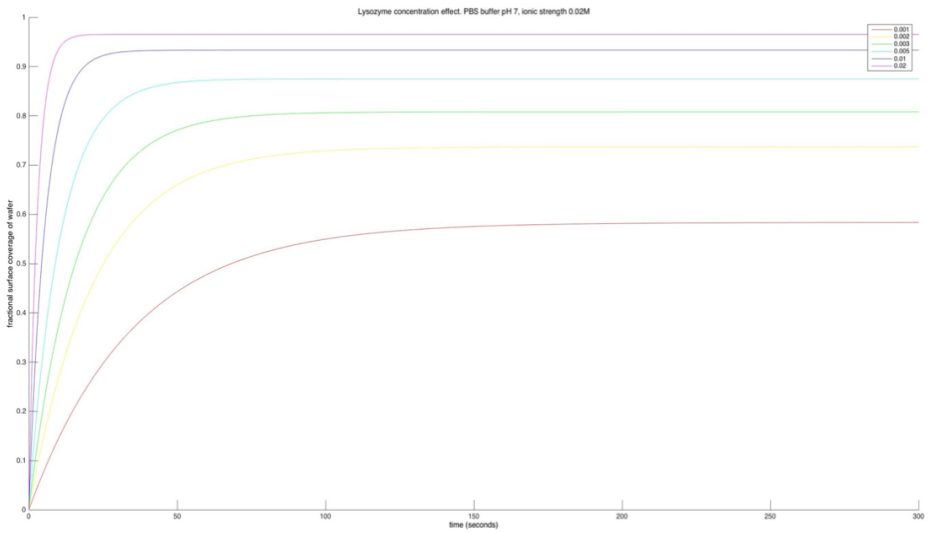

Figure 13: lysozyme concentration effect fractional surface coverage prediction for the range of 0.001 to 0.02 mg/ml

Figure 13 shows the simulations predictions of the concentration effect for lysozyme. The trend is positively correlated, where an increase in lysozyme concentration causes an increase in fractional coverage of the wafer. This is intuitive and the predictions trend agrees with the experimental data. The model also predicts a convergence towards an upper limit as each increase in concentration results in a smaller increase in adsorbed amount. At a concentration of $0.02 mg ml^{-1}$ the surface coverage is predicted to be almost 100%.

2. The pH Effect

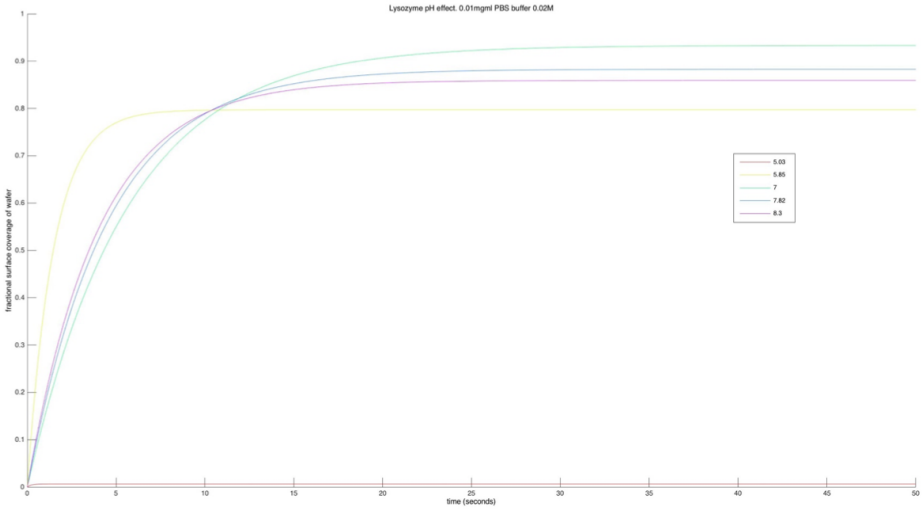

Figure 14: The pH effect on lysozyme 0.01mg/ml for a range of pH value from 5.03 to 8.3

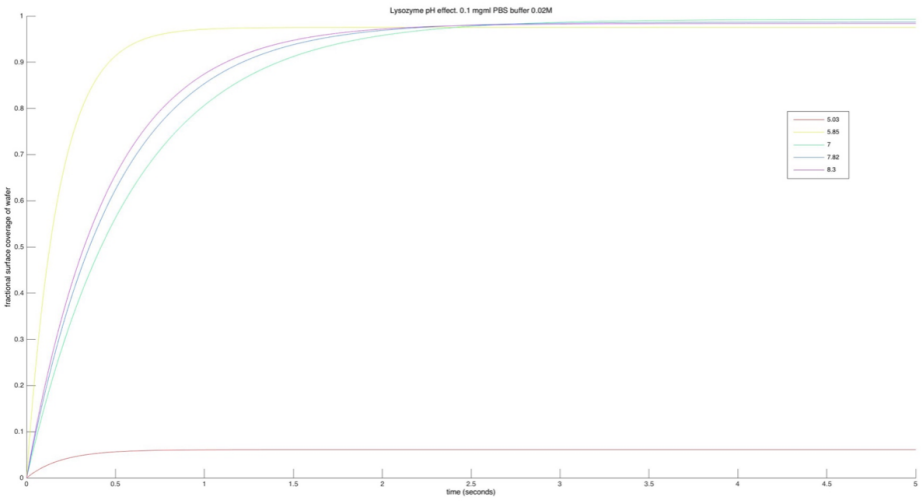

Figure 15: The pH effect on lysozyme 0.1 mg/ml for a range of pH value from 5.03 to 8.3

The pH effect for a lysozyme concentration of $0.01 mgml^{-1}$ is shown in figure 14, the model predicts an adsorption preference towards a neutral

pH value, with the greatest surface cover occurring at a pH of 7. This prediction agrees with the experimental data recorded for $0.01 mgml^{-1}$ lysozyme concentration. The pH effect for a lysozyme concentration of $0.1 mgml^{-1}$ is shown in figure 15, the model predicts a general positive trend, an increase in pH results in an increase in adsorbed amount. This trend agrees with the experimental data. However, a pH value of 5.85 is predicted to provide the greatest value of adsorption, this was not observed in the experimental data.

3. The Ionic Effect

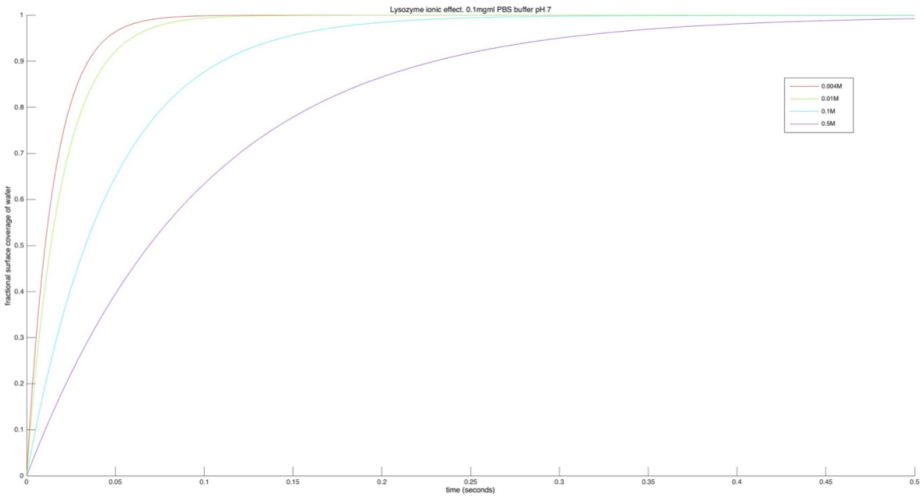

Figure 16: Ionic effect on lysozyme 0.1mg/ml

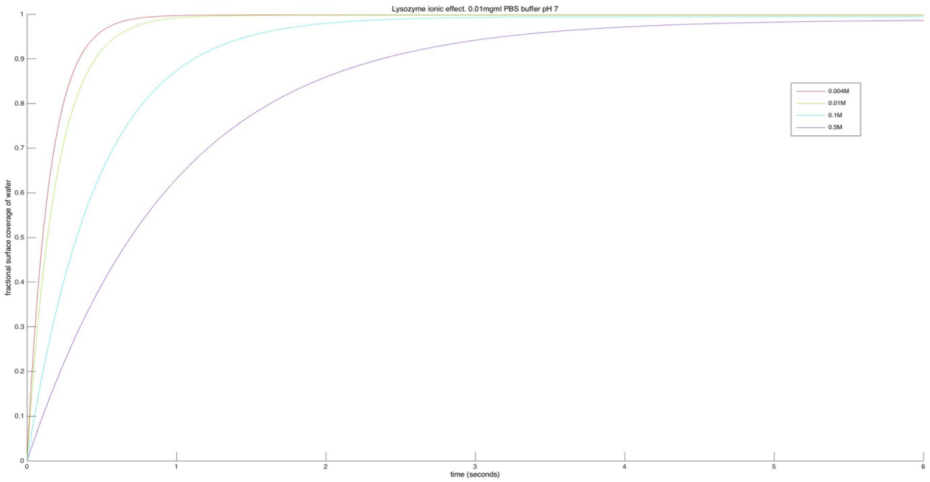

Figure 17: Ionic effect on lysozyme 0.01 mg/ml

Figures 16 and 17 show the ionic effect predictions for lysozyme concentrations of 0.1 and $0.01 mgml^{-1}$ respectively. A negative correlation is predicted for both lysozyme concentrations with respect to an increase in ionic strength. The greatest surface coverage predicted is observed for an ionic strength of $4mM$. This trend prediction agrees with the experimental findings for the ionic effect on lysozyme.

4.3. Discussion

The results of adsorption obtained from ellipsometry reveal that lysozyme and BSA adsorption obey the same positive trend relating an increase in protein concentration to an overall increase in protein adsorption amount. The results show a substantial different between the adsorption affinity between the two proteins, showing that lysozyme is the most prone to adsorb. The data also revealed that lysozyme and BSA adsorption obey opposite correlations to changes in pH and ionic strengths. Positive correlations were found for the amount of BSA adsorption corresponding to increases in pH and ionic strength. While lysozyme adsorption showed a negative correlation for the same increases in pH and ionic strength. The hypothesis behind these opposing correlations is the relation between pH and the isoelectric point of the protein. The isoelectric point for lysozyme is at a pH of 10.7 while that of BSA is at a pH of 4.8. This means at neutral pHs the two proteins will be oppositely charged and will be effected oppositely to the same change in

pH within the pH range of 4.8 to 10.7. Within the simulation a few issues became evident in the predictions it makes. The first major issue is with the inaccurate BSA ζ potential value, this led to an error and subsequently no predictions were made for BSA. A possible solution for this would be the application of the Lindstorm-Lang equation and Gouy Chapman equation to mathematically derive the BSA ζ potential value [18].

The simulation also lacked the ability to replicate the irreversible adsorption of proteins and the continuous adsorbing and escaping of the reversibly bound proteins, which causes the distinctive wobble seen in the graphs plotted from ellipsometry data. The implementation of a Langmuir adsorption model which would represent the wafer as a grid of binding sites, upon protein collision with one of these sites it could either bind irreversibly, reversibly or not bind. However, the Langmuir was only contemplated and never implemented due to time constraints of the project.

5. Conclusion

The general trends seen in the experiment and simulation, correlated fairly well with each other as well as being in agreement with the extensive amount of previous results produced for lysozyme and BSA adsorption. It was shown that lysozyme has a much greater affinity to adsorb than BSA across all experiments. The pH and ionic effects showed opposite trends for lysozyme and BSA, these trends supported the theoretically prediction made by the underlying microscopic interaction between the ions. The predictions produced from the simulation had good and bad aspects to them, overall the simulation delivered great insight into the powerful ways in which the complex process of protein adsorption can be mathematically described. Although the units and scaling associated with the simulation data produced were meaningless the trends produced agreed with the experimental trends. Future work is necessary to correctly produce meaningful simulation data that matches that of the ellipsometry data already distinguished. Alternative mathematical methods and the potential of other models have been contemplated but not implemented due to time constraints. The most promising alternative simulation method would be that of a Langmuir adsorption grid.

References

[1] Ramsden, J. J. and Prenosil, J. E. (1994) Effect of Ionic Strength on Protein Adsorption Kinetics. J. Phys. Chem. 98, 5376 5381.

[2] Beverung, C. J. et al. (1999) Protein adsorption at the oil/water interface: characterization of adsorption kinetics by dynamic interfacial tension measurements. Biophysical Chemistry 81, 1999, pp 59-80.

[3] Dickinson, E. (1991) A Statistical Model for the Simulation of Adsorption from a Mixture of Deformable Particles. Procter Department of Food Science, University of Leeds

[4] Azzam, R. M. A. (2010) Handbook of optics: Volume 1 Geometrical and Physical Optics, Polarized Light, Components and Instruments Third Edition Chapter 16: Ellipsometry. The McGraw-Hill companies, Inc. ISBN: 978-0-07-162925-4

[5] Lu, J. R. Murphy, E. F. et al. (2000) Characterization of Protein Adsorption at the Phosphorylcholine Incorporated Polymer-Water Interface. Macromolecules 2000, vol. 33, pp 4545-4554.

[6] Lu, J. R. Gilchrist, V. A. (1999) Adsorption of Penta(ethylene glycol) Monododecyl Ether at the Solid Poly(methyl methacrylate)-Water Interface: A Spectroscopic Ellipsometry study. Langmuir 2000, Vol. 16, pp 740-748.

[7] 7. The Editors of Encyclopdia Britannica. Encyclopdia Britannica. [place unknown]: Encyclopdia Britannica; 2016 Apr 18. Snells law — physics; [cited 2016 Sep 15]. Available from: https://www.britannica.com/science/Snells-law.

[8] Inc EO. Optics - imaging - Photonics - Optomechanics - lasers; 1942 [cited 2016 Sep 15]. Available from: http://www.edmundoptics.com/.

[9] J.A. Woollam Co. Ellipsometry Tutorial - J.A. Woollam Co; 2016 [cited 2016 Sep 15].
Available from: https://www.jawoollam.com/resources/ellipsometry-tutorial.

[10] El-Agez TM, Taya SA, El Tayyan AA. An Improvement of Scanning Ellipsometer by Rotating a Polarizer and an Analyzer at a Speed Ratio of 1:3. International Journal of Optomechatronics March 2011. 2011 Mar.

[11] Biological magnetic resonance bank; 2008 [cited 2016 Sep 15]. Available from: http://www.bmrb.wisc.edu/featuredSys/Lysozyme/index.shtml.

[12] SIGMA-ALDRICH, inc. Product Information: Bovine serum albumin (A0281). 1990.

[13] Palacio, L. et al. (2003) Fouling with protein mixtures in microfiltration: BSA-lysozyme and BSA-pepsin. Journal of Membrane Science 222, pp 41-51.

[14] Stone E. Texas A&M University. Gibbs free energy [2016 Sep 15]. Available from: https://www.chem.tamu.edu/class/majors/tutorialnotefiles/gibbs.htm.

[15] Van Oss, C. (1994) Interfacial Forces in Aqueous Media. Marcel Dekker, Inc. ISBN: 0- 8247-9168-1 pp 1,14,15,20

[16] Cail, T. Hochella, F. Jr. (2003) Chapter 3 The effects of solution chemistry on the sticking efficiencies of viable Enterococcus Faecalis: an atomic force microscopy and modelling study. Virgina polytechnic Institute and State University.

[17] IUPAC gold book - electrokinetic potential, ; 2014 Feb 24 [2016 Sep 15]. Available from: http://goldbook.iupac.org/E01968.html.

[18] Cacace, M. Landau, E. Ramsden, J. (1997) The Hofmeister series: salt and solvent effects on interfacial phenomena. Quarterly Review of Biophysics. pp 257,258,262. Vol. 30.

[19] Spielman, L. Friedlander, S. (1974) Role of the Electrical Double Layer in Particle Deposition by Convection Diffusion. Journal of Colloid and Interface Science. Vol. 46. Issue 1. Pages 22-31.

[20] User S. Zeta potential, short tutorial; 2013 [cited 2016 Sep 15]. Available from: http://www.dispersion.com/zeta-potential-short-tutorial.

[21] Van Oss CJ, Chaudhury MK, Good RJ. Interfacial Lifshitz-van der Waals and polar interactions in macroscopic systems. Chemical Reviews. 1988 Sep;88(6):92741.